

Multi-pass Gaussian Contact-hardening Soft Shadows

Kevin Cherry and Robert Kooima

Center for Computation and Technology, Louisiana State University, Baton Rouge, Louisiana, U.S.A.

Keywords: Real-time Soft Shadows, Contact-hardening Shadows, Variable-sized Penumbrae, Post-process Soft Shadows.

Abstract: Real-time soft shadows have seen numerous improvements over the years. Post-process blurring of shadow edges are commonly used to hide aliasing artifacts, but in some cases, such as ours, it is used to mimic physical processes. Instead of generating penumbra regions uniformly, we scale key algorithmic components in screen space to allow the penumbra region to grow in accordance with occluder/receiver distance. This form of soft shadowing is known to some as contact-hardening and has been explored in various ways. We present an algorithm that explores three ways of achieving contact-hardening soft shadows. Two of those ways are similar in nature to previous works while the third is a novel approach that utilizes occluder distance as a counter for multiple Gaussian passes. Our main contributions are fast occluder approximation and the use of occluder distance to control the number of Gaussian passes. Multiple Gaussian passes create better results than a single Gaussian pass for several scenes, and we explore various ways of improving the performance of the multi-pass approach.

1 INTRODUCTION

There have been many different shadow algorithms created over the years, however most of them stem from two main approaches; that of shadow maps (Williams, 1978) and shadow volumes (Crow, 1977). Here we focus on the former, shadow maps. Standard shadow maps can only generate hard shadows, that is, fragments are either completely lit or completely in shadow. The region completely in shadow is known as the umbra. The region partially shadowed that forms a gradient from shadowed to lit is known as the penumbra. More sophisticated shadow map algorithms are generally concerned with better utilization of map resolution, the use of soft shadow techniques strictly to hide aliasing artifacts, or, in our case, the use of soft shadow techniques for greater scene realism. Our approach focuses on creating variable penumbra widths that scale with occluder distance. Toward this end we present one main algorithm with three alterations and compare this to previous work in the field. Two of our approaches require only one pass. One of them uses a PCF filter and the other a Gaussian filter. Our main alteration uses multiple Gaussian passes. The occluder distance controls the number of passes. The size of the kernel can either be fixed or vary with each pass and the standard deviation of the kernel is linked to that size via the 3-sigma rule, which enforces that sigma be equal to size

divided by three. We use a Poisson disk distribution with a custom number of taps to control where we sample the Gaussian kernel. It is important to note that this value is separate from kernel size. As kernel size increases, the taps expand to cover the new area. All three operate in screen space as a post process over what we call a *distance map*. The resulting information in this map is then used to generate the shadow regions in the final pass.

2 RELATED WORKS

2.1 Soft Shadows

Percentage closer filtering (Reeves et al., 1987) is the most common soft shadow technique. Instead of considering only the current fragment, we consider the neighborhood of the fragment (an area known as a box filter or kernel) and calculate the percentage of neighboring fragments that are in shadow. If the percentage is zero, the pixel is lit. If the percentage is one, the pixel is in the umbra of the shadow. Any percentage in between indicates the pixel is in the penumbra and the percentage determines how dark the pixel appears. For example, if we examine a 3×3 neighborhood around the pixel (8 taps other than the pixel itself) and 3 of its neighbors are lit (i.e. have a

value of zero) while the pixel itself and its 5 remaining neighbors are in shadow (i.e. have a value of one), then the final percentage for the pixel in the center is $3/9$ or 33% in shadow. In our experience, PCF produces visually satisfying results, but a kernel size of 4×4 or 5×5 is required. This increases the number of taps quadratically since, given a square kernel of size N , each pixel requires N^2 shadow map references. In contrast, both of our Gaussian algorithms require $2N$ taps due to the separable nature of a Gaussian kernel.

Variance shadow maps (Donnelly and Lauritzen, 2006) store not just the depth from the point of view of the light source, but also the depth squared, or second moment of the depth value, in a separate channel. These values are used in the main rendering pass to compute the mean and variance over a filter region. Chebychev's inequality (Theorem 1 and Equation 5 in (Donnelly and Lauritzen, 2006)) is then used to estimate an upper bound on the percentage of pixels in the filter region that are in shadow (the same value computed by a PCF filter). This ultimately determines the darkness of the penumbra at that pixel as the light intensity can be scaled by this value. To avoid sampling all points in the filter region, one can apply a Poisson disk distribution to choose a small subset of samples to represent the entire region. One can also use a pre-filtering technique such as a Gaussian blur for smoother results. It is interesting to note that very little extra calculation and memory overhead are required, yet satisfying soft shadows are generated. This approach works for different types of lights. The soft shadow results, however, have uniform width irrespective of occluder distance or other contact-hardening criteria.

2.2 Contact-hardening Soft Shadows

(Wyman and Hansen, 2003) use what they call "penumbra maps" to calculate soft shadows. They take the typical shadow map approach to generate depth values from the point of view of the light source. They then generate a second texture, the penumbra map, by finding the silhouette edges and expanding them using cones on the vertices and sheets connecting these cones along silhouette edges. The final scene is then rendered using the shadow and penumbra maps. This approach assumes a spherical light source, however different light shapes are supported. Though not described in these terms, this approach does create contact-hardening results.

Expanding on the PCF approach described above, the Percentage-Closer Soft Shadow (PCSS) (Fernando, 2005) algorithm creates contact-hardening shadows by varying the PCF kernel size at each frag-

ment in accordance with the size of the light source and distance from the occluder. This is similar to our pcf approach, however PCSS uses the light's size as well as a more complex occluder search algorithm. For our approach, light size is not taken into account and only occluder distance is used, as obtained from the original shadow map. We also use an approximation of occluder-receiver distance.

Since algorithms like PCF and PCSS require many texture lookups, (Gumbau et al., 2010) describe an algorithm that uses a separable Gaussian kernel, requiring fewer lookups. They call their approach Screen Space Soft Shadows (SSSS). Our approaches are also performed in screen space and the technique described by SSSS is similar to our single pass Gaussian approach. However in our multi-pass approach, as mentioned earlier we use a Poisson disk distribution to reduce the total number of taps to a constant, kernel size agnostic value. This also allows us to render the scene once per blur as opposed to twice; once for horizontal and once for vertical. This further allows us to explore much bigger kernel sizes.

Multi-View Soft Shadowing (MVSS) (Bavoil, 2011) was created by nVidia. This approach uses multiple shadow maps from different points on an area light source. These points are chosen using a Poisson disk sampling pattern. For each pixel, each shadow map is queried and an average over all maps is taken. This average controls the strength of the shadow at that pixel. PCF with a constant kernel size of 2×2 is applied to all shadow map references.

(Klein et al., 2012) use an erosion operator. They first generate classic hard shadows, then perform edge detection with a Laplacian kernel. For those pixels detected to be shadow edges, the occluder and camera distance are stored in separate channels. This information is then used to calculate penumbra width, which in turn is used to scale an erosion kernel applied in the next pass. The final pass can use PCF with a kernel size also scaled by the penumbra width.

3 ALGORITHM

The main algorithm is described in detail below in text and pseudocode. We explore three variations: PCF with a variable-sized kernel, single pass Gaussian blur with a variable-sized kernel, and a multi-pass Gaussian blur with a fixed or variable-sized kernel with occluder distance guiding the number of Gaussian passes performed.

3.1 Description

Our algorithm begins in the first pass whereby the standard shadow map is created by rendering only the depth information of the scene from the point of view of the light source into a depth buffer.

The next pass renders from the point of view of the camera. Here we perform the normal rendering pass that would generate hard shadows from the previously collected shadow map. However, instead of drawing fragments either lit or shadowed, we save this binary value into one of the channels of our distance map (0 for lit, 1 for shadowed) along with the distance to the occluder in another channel. The distance to the occluder is simply the difference between the distance of the current fragment (projected into light space) to the light source and the value looked up in the shadow map. The distance is raised to a user-specified power and then multiplied by a user-specified value. This is done to help control how sharply the penumbra portion grows and how long the contact-hardening portion lasts before spreading into a penumbra region. These values should scale with the general size of the scene and estimated occluder distance. When figuring out the proper value for these two variables, it helps to draw the occluder distance into the scene via a color gradient so one can visually examine the modified occluder distance to ensure a proper progression of penumbra scale.

The third pass is optional and depending on the scene, it can help areas where shadows form thin lines on the receiver. It can also help to expand the penumbra such that both an outer and inner penumbra region is visible. This pass dilates the occluder distance values found in the distance map that was written during the second pass. Simply apply a Gaussian filter over the channel to expand the penumbra region in later passes.

Pass four is where the three alterations come into play. The first alteration uses a PCF filter to modify the binary shadow value from our distance map using the occluder distance to control filter size. The second alteration is similar but uses a Gaussian filter to modify the shadow value and uses the occluder distance to control the size of the Gaussian kernel. The last alteration performs multiple Gaussian blur passes modifying the shadow value and decreasing the occluder distance with each pass. Those fragments with an occluder distance that has been decremented to zero (or started out at zero) do not get blurred for all subsequent passes. The kernel size can either be fixed or can be upper bounded with the first pass starting at small values (e.g. size of 3x3) and can increase with each pass until reaching the upper bound. This will

speed up the multi-pass part. We precompute up to 64 two-dimensional Poisson points in the inclusive range of -1 to +1. The first point is fixed at the origin so the center texel is always examined. After the first point, the Poisson algorithm proceeds as usual to create a valid Poisson distribution. Before we make our blur pass, we take from the first of these Poisson points up to the desired amount and use these as (x, y) offsets into our Gaussian kernel. We compute these Gaussian weights for each offset and then normalize them. Each offset along with its corresponding Gaussian weight is sent to the shader. Once in the fragment shader, we need only loop through the values given. For each iteration, we add the offset to the current fragment location in screen space and sample the distance map at that point. We then multiply it by the normalized Gaussian value and add this to our cumulative total. After the loop, this total is written back into the distance map as the new shadow value.

The final pass renders the scene normally and uses the modified, previously binary, shadow value from the distance map with 0 meaning the fragment is lit, 1 meaning the fragment is part of the umbra region, and values in between specifying the intensity of the penumbra region.

3.2 Pseudocode

Pass 1:

Render the shadow map normally.

Pass 2:

Compare fragment against shadow map.

Let S be 0 if fragment is lit, 1 otherwise.

Let D be (occluder distance) ^{D_p} · D_m , where

D_p is the distance power

D_m is the distance multiplier

Write S and D into different channels in the distance map.

Pass 3 (Optional):

Dilate all D values using a Gaussian kernel.

Write new values back into the distance map.

Pass 4:

Choose one of the following and do for each fragment, then write results back into the distance map:

- **PCF:**

Apply PCF to S value using D to control kernel size.

Write new S value.

- **Single Pass:**

Apply Gaussian filter to S value using D to control kernel size.

Write new S value.

- **Multi-Pass:**

For each pass up to a specified limit:

If $D > 0$:

Let KS be the kernel size, which is either fixed or progressively widening with each pass.

Let P be the set of precomputed 2D Poisson disk points we wish to use.

For each P_i in P :

Calculate the Gaussian weight.

Multiply P_i by KS to get the texture offset.

Normalize all Gaussian weights.

Send texture offset and normalized Gaussian weight for all P_i to the shader.

Render using sent data to apply the Gaussian filter to blur all S values

Decrement all D values

Write new S value

Write new D value

Pass 5:

Render scene normally.

Read from the distance map.

If $S = 0$

Fragment is lit.

Else if $S = 1$

Fragment is in shadow.

Else fragment is in penumbra with intensity S .

4 RESULTS

We created a project using C# and the .Net OpenGL port called SharpGL. We implemented various soft shadow algorithms in addition to our own. All code was run on a Windows machine with an nVidia Geforce GT 630M card with 2GB of GPU memory.

4.1 Test Scenes and Timings

Table 1 lists various information about the test scenes we use including the count of vertices, triangles, and meshes. We try to use a variety of scene sizes to better test the speed of our algorithms. Since the exact way in which a model is rendered (i.e. the implementation decisions) can affect performance regardless of

Table 1: Test scene statistics including total number of vertices, triangles, and separate meshes.

Scene Name	Vertices	Triangles	Meshes
Fence	16	24	2
Ball	880	1,752	2
Log Cabin	1,407	2,630	13
Pool	8,463	11,003	1

Table 2: This data shows the approximate time taken to render a single frame in milliseconds for different algorithms using the Pool scene.

Algorithm	Frame Time
PCF approach	17
Single pass Gaussian	20
Multi-pass Gaussian	18

the particular shadow algorithm used, we also provide comparative results to better show the differences in speed based more on algorithm complexity and less upon raw speed of model rendering. Table 2 shows the raw frame timings calculated in milliseconds using the Pool scene of different algorithms. All timings done using OpenGL queries so as to get the actual time spent on the GPU.

4.2 Visual Results

We now show the results of executing our algorithm and other soft shadow techniques on the different scenes mentioned above. Since the main objective of our algorithm is better realism through contact-hardening soft shadows and not better utilization of map density, each shadow map was given a resolution of 2048x2048 so as to mostly eliminate aliasing artifacts. When comparing algorithms, each algorithm was given parameters that resulted in the best results for that scene.

In Figure 1 we visually compare the results of the different approaches on the Pool scene. We compare the PCF, single Gaussian pass, and multiple Gaussian pass approaches from our algorithm. The palm tree leaves are simply quads with a texture using the alpha channel to denote the areas between the leaves.

Figure 2 shows the effects of the dilate pass. We used the PCF approach on the Fence scene to show how using the dilate pass may not always be best depending on the scene. In this case, the outer penumbra created by the dilate pass causes the shadow to be overly blurry and thicker than they should be. Also in areas with dense thin shadow lines, the dilate pass can cause the lines to merge, thereby losing some of their detail. Sometimes this can be desirable and lead to realistic results, so each scene should be examined carefully before deciding whether to use this pass.

We examine the Fence scene again in Figure 3. Here we show all three approaches of our algorithm. In the PCF approach the shadow transitions too harshly from hard to soft shadows and this causes a noticeable change in shadow intensity. The single pass approach is too light at the base of the fence. The multi-pass approach combines consistent shadow intensity with a smooth transition from hard to soft shadows.

Figure 4 shows how the penumbra grows along with the occluder distance. The scene is shown with the penumbra clearly marked with a dark gradient. The umbra portion is inside of the gradient.

In Figure 5 we show the effects of multiple algorithms on a simple elongated shadow cast in the Ball scene. From left to right we examine hard shadows, uniform Gaussian blur soft shadows, PCF with two different settings, and our contact-hardening approach with PCF, then single pass Gaussian, and finally our multi-pass Gaussian approach.

We examine the effect of changing the number of Poisson points used to sample our Gaussian kernel in Figure 6. For small kernels less points are needed to sufficiently cover the area and provide an adequate approximation. As the kernel increases in size, more points are needed to keep a decent approximation. In Figure 7 we further examine the effects the number of Poisson points have. Here we use a 29x29 Gaussian kernel and varying the number of points from 1 to 20. Even with a small number of points on such a large kernel, the results quickly approximate the effects of sampling the entire Gaussian.

Figure 8 shows our Log Cabin scene without textures to better show the shadows. Figure 9 is a close up of the wooden poles by the cabin. This shows the transition from hard to soft shadows.

5 DISCUSSION

Our first approach, using PCF as a filter, is similar to PCSS and produces decent results. Our second approach, using a Gaussian filter in a single pass, is similar to SSSS. Our third approach, using a Gaussian filter in multiple passes, produces the best results in our test scenes. The fastest of these is the single pass approach, however if the max number of Gaussian passes in the multi-pass approach is limited to small numbers, it too can achieve interactive speeds. Since the number of Poisson taps is constant and independent of kernel size, we can use bigger kernels at faster speeds than a separable Gaussian approach. Kernel size can start small and increase with each pass thereby making it even faster but still achieving great

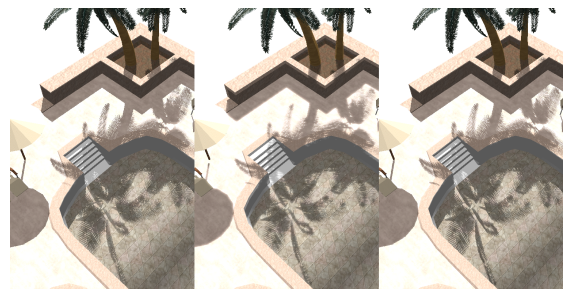


Figure 1: This shows the difference between the three approaches. All approaches use a 2048x2048 map. (left) Using PCF as the filter, (center) using single pass Gaussian as the filter, (right) using multi-pass Gaussian as the filter. The PCF approach appears too sharp in many areas and has leaves where the needles seem to go from light to dark causing a disturbing pattern. The single pass Gaussian is too blurred in many areas and as such it loses a lot of detail. The multi-pass approach shows the detail in the leaves and still allows for a soft blur around the needles.

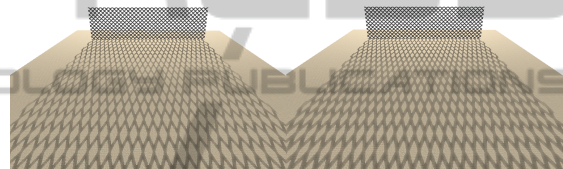


Figure 2: Our PCF approach without (left) and with (right) a pre-filter dilation over the distance map. This shows that sometimes Pass 3 from the algorithm is harmful to the final result. In the above case we have unrealistically thick lines in the shadow. Therefore Pass 3 should be omitted in this scene. The specific scene and approach must be considered before deciding whether to use the dilation in Pass 3 or not.

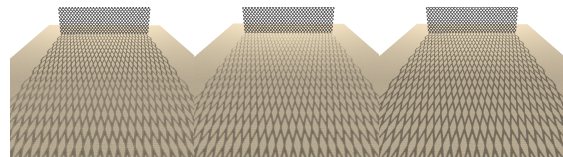


Figure 3: This shows the difference between the three approaches. (left) Using PCF as the filter, (center) using single pass Gaussian as the filter, (right) using multi-pass Gaussian as the filter.

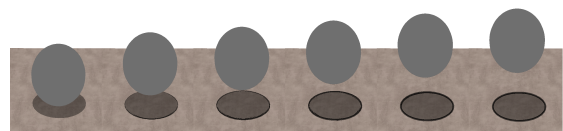


Figure 4: We have coded in the shader a special penumbra type that clearly distinguishes umbrae from penumbrae regions. The dark lines indicate penumbra and the shaded portion within is the umbra. Here we see as the ball gets higher in the air and therefore further from the receiver, its penumbra region grows.

results.

There are two main parts to any penumbra, the in-

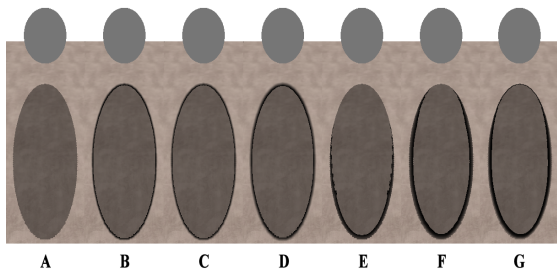


Figure 5: Comparison of several algorithms using the Ball scene. The ball's shadow is elongate and the penumbra region is clearly marked as in Figure 4 so as to show the effects of the contact-hardening algorithms. A) Normal hard shadows. B) Uniform Gaussian blur using kernel size of 5×5 . C) Uniform PCF with kernel size of 5×5 . D) Uniform PCF with kernel size of 7×7 . E) Our own PCSS-like approach with no dilation and dynamic kernel size ranging from 1×1 (i.e. no filter) up to 19×19 . D_p was set to 3.0 and D_m was set to 200. F) Our own single pass Gaussian approach without dilation and dynamic kernel size ranging from 1×1 up to 19×19 . D_p was set to 1.9 and D_m was 200. G) Our own multi-pass Gaussian approach without dilation and a maximum of 10 Gaussian passes. Each successive pass increased the kernel size starting from 3×3 and going up to 19×19 with 20 Poisson taps. D_p was 3.0 and D_m was 200. The contact-hardening approaches in E, F and G are more realistic than the uniform soft shadow approaches. The multi-pass approach in G achieves the best results and uses the smallest number of taps among the contact-hardening approaches.

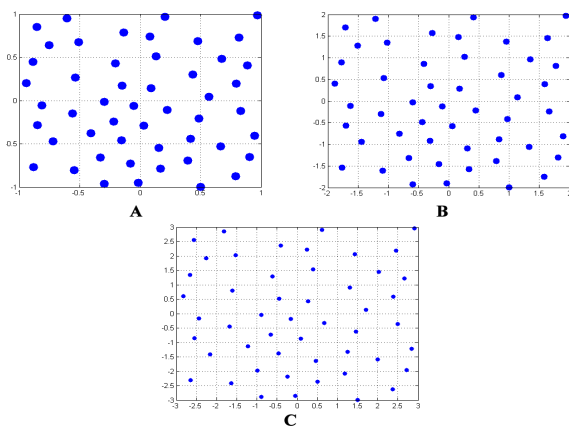


Figure 6: This shows the coverage of 50 Poisson points in a Gaussian kernel. As the size of the kernel increases, the space between the points increase and coverage becomes more sparse. The number of points need to be chosen such that the total coverage is sufficient. One can use less taps than that of a separable Gaussian approach and still receive satisfactory results. A) Kernel size of 3. Points go from -1 to +1. B) Kernel size of 5. C) Kernel size of 7.

ner and the outer penumbra. The inner penumbra is the part that would be an umbra fragment in a hard shadow algorithm but instead has its color brightened to represent a part of the penumbra. The outer penum-

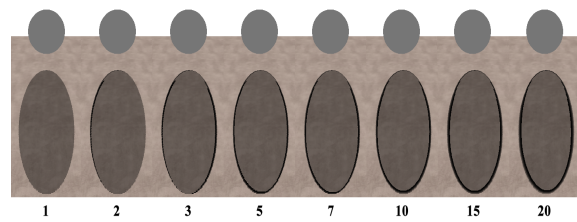


Figure 7: This is our multi-pass approach with 10 passes and varying amounts of Poisson points used for a 29×29 Gaussian kernel. The number of points used is under each image. We fix the first point at the origin, allowing the first sample to be at the center.



Figure 8: Our multi-pass approach with a 4096×4096 shadow map shown without textures for better shadow clarity.

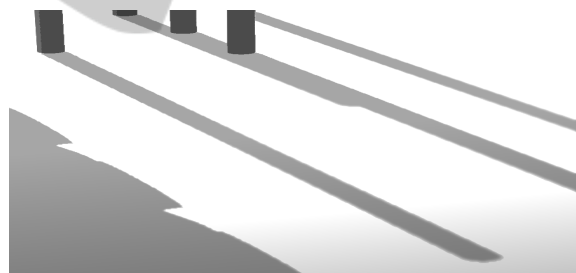


Figure 9: Closeup of the multi-pass Gaussian showing the transition from hard to soft shadows.

bra is the part that would be lit and right next to the umbra in a hard shadow algorithm but instead has its color darkened to represent a part of the penumbra. In the multi-pass algorithm, the dilate pass mostly controls the outer penumbra, as it mainly causes the hard shadow edges to grow outward. The multiple Gaussian passes after this control the inner umbra, as they only lighten the color of already shadowed pixels, i.e. lit pixels are untouched. It is important to know this distinction so one can make informed decisions about such aspects as choosing a proper kernel size for the dilate pass and choosing the max kernel size for the Gaussian multi-pass.

There is an optimization for the multi-pass approach whereby another pass is added right before the

dilate pass. This pass examines a neighbor around each pixel, that is at least as big as the max kernel size for the Gaussian pass, and inspects each neighbor's S value. If all neighbors, including the center pixel, are in shadow, the D value for the center pixel is changed to zero. The purpose of this is to detect pixels that are deep inside the umbra of a shadow and therefore should be skipped during all Gaussian blur passes. This greatly increases the speed of the algorithm, however this has side effects. Since the Gaussian passes are responsible for creating the inner penumbra, if a pixel is chosen that would have normally been blurred by later passes, then that pixel becomes immune to any blur passes. This means the pixels closest to the hard shadow edge that are chosen to be part of the inner umbra and have their D values set to zero, are the pixels where the inner penumbra cannot grow past. Therefore a kernel bigger than the max kernel size must be chosen for this pass in order to not restrict how deep the inner penumbra grows. As the kernel size grows for this pass, the time savings diminish. Care must be taken when using this optimization.

Since this is a post-process algorithm, other algorithms can be combined to achieve greater results. For example, our objective is not to increase nor better utilize shadow map density. Therefore techniques such as Cascaded Shadow Maps (Dimitrov, 2007), Light Space Perspective Shadow Map (Wimmer et al., 2004), Sample Distribution Shadow Maps (Lauritzen et al., 2011), and others can be used to greatly reduce aliasing before applying our algorithm.

6 FURTHER WORK

Other low-pass filters can be used in place of a Gaussian kernel. We have not explored as to whether there are benefits of using these other types of kernels.

The kernel shape may benefit from taking into account the shape of the light source. While the kernel size is dynamic according to occluder distance for two of the stated approaches, light size can still perhaps influence the initial kernel size or the rate of kernel size growth. The light's size can also have an effect on the multi-pass approach. These may lead to more accurate shadows with respect to different types of area lights. This will also allow us to calculate penumbra width based on the well known formula from (Fernando, 2005):

$$\omega_{penumbra} = \frac{(d_{receiver} - d_{blocker}) * \omega_{light}}{d_{blocker}}$$

where ω is width and d is distance. We could also incorporate observer distance as in (Klein et al., 2012) by modifying the equation to be:

$$\omega_{penumbra} = \frac{(d_{receiver} - d_{blocker}) * \omega_{light}}{d_{blocker} * d_{observer}}$$

Although we do not believe this to have a huge impact on accuracy, the case of having more than one occluder has not been extensively tested. We could incorporate and test an average or min occluder depth algorithm.

REFERENCES

- Bavoil, L. (2011). Multi-view soft shadows. Technical report, NVIDIA, technical report, <http://developer.nvidia.com>.
- Crow, F. C. (1977). Shadow algorithms for computer graphics. In *ACM SIGGRAPH Computer Graphics*, volume 11, pages 242–248. ACM.
- Dimitrov, R. (2007). Cascaded shadow maps. *Developer Documentation, NVIDIA Corp.*
- Donnelly, W. and Lauritzen, A. (2006). Variance shadow maps. In *Proceedings of the 2006 symposium on Interactive 3D graphics and games*, pages 161–165. ACM.
- Fernando, R. (2005). Percentage-closer soft shadows. In *ACM SIGGRAPH 2005 Sketches*, page 35. ACM.
- Gumbau, J., Chover, M., and Sbert, M. (2010). *Screen Space Soft Shadows*.
- Klein, A., Nischwitz, A., and Obermeier, P. (2012). Contact hardening soft shadows using erosion.
- Lauritzen, A., Salvi, M., and Lefohn, A. (2011). Sample distribution shadow maps. In *Symposium on Interactive 3D Graphics and Games*, pages 97–102. ACM.
- Reeves, W. T., Salesin, D. H., and Cook, R. L. (1987). Rendering antialiased shadows with depth maps. In *ACM SIGGRAPH Computer Graphics*, volume 21, pages 283–291. ACM.
- Williams, L. (1978). Casting curved shadows on curved surfaces. In *ACM Siggraph Computer Graphics*, volume 12, pages 270–274. ACM.
- Wimmer, M., Scherzer, D., and Purgathofer, W. (2004). Light space perspective shadow maps. In *Proceedings of the Fifteenth Eurographics conference on Rendering Techniques*, pages 143–151. Eurographics Association.
- Wyman, C. and Hansen, C. D. (2003). Penumbra maps: Approximate soft shadows in real-time. In *Rendering Techniques*, pages 202–207.